Clinical Proteomics

RESEARCH

Open Access

Characterizing age-related changes in intact mitochondrial proteoforms in murine hearts using quantitative top-down proteomics

Andrea Ramirez-Sagredo[1†], Anju Teresa Sunny[2†], Kellye A. Cupp-Sutton[2], Trishika Chowdhury[2], Zhitao Zhao[3], Si Wu[2,3*] and Ying Ann Chiao[1*]

Abstract

Background Cardiovascular diseases (CVDs) are the leading cause of death worldwide, and the prevalence of CVDs increases markedly with age. Due to the high energetic demand, the heart is highly sensitive to mitochondrial dysfunction. The complexity of the cardiac mitochondrial proteome hinders the development of effective strategies that target mitochondrial dysfunction in CVDs. Mammalian mitochondria are composed of over 1000 proteins, most of which can undergo post-translational modifications (PTMs). Top-down proteomics is a powerful technique for characterizing and quantifying proteoform sequence variations and PTMs. However, there are still knowledge gaps in the study of age-related mitochondrial proteoform changes using this technique. In this study, we used top-down proteomics to identify intact mitochondrial proteoforms in young and old hearts and determined changes in protein abundance and PTMs in cardiac aging.

Methods Intact mitochondria were isolated from the hearts of young (4-month-old) and old (24-25-month-old) mice. The mitochondria were lysed, and mitochondrial lysates were subjected to denaturation, reduction, and alkylation. For quantitative top-down analysis, there were 12 runs in total arising from 3 biological replicates in two conditions, with technical duplicates for each sample. The collected top-down datasets were deconvoluted and quantified, and then the proteoforms were identified.

Results From a total of 12 LC-MS/MS runs, we identified 134 unique mitochondrial proteins in the different sub-mitochondrial compartments (OMM, IMS, IMM, matrix). 823 unique proteoforms in different mass ranges were identified. Compared to cardiac mitochondria of young mice, 7 proteoforms exhibited increased abundance and 13 proteoforms exhibited decreased abundance in cardiac mitochondria of old mice. Our analysis also detected PTMs of mitochondrial proteoforms, including *N*-terminal acetylation, lysine succinylation, lysine acetylation, oxidation, and phosphorylation. Data are available via ProteomeXchange with the identifier PXD051505.

†Andrea Ramirez-Sagredo and Anju Teresa Sunny contributed equally to this work.

*Correspondence:
Si Wu
swu49@ua.edu
Ying Ann Chiao
ann-chiao@omrf.org

Full list of author information is available at the end of the article

Conclusion By combining mitochondrial protein enrichment using mitochondrial fractionation with quantitative top-down analysis using ultrahigh-pressure liquid chromatography (UPLC)-MS and label-free quantitation, we successfully identified and quantified intact proteoforms in the complex mitochondrial proteome. Using this approach, we detected age-related changes in abundance and PTMs of mitochondrial proteoforms in the heart.

Keywords Top-down proteomics, Label-free quantitation, Post-translational modifications, Mitochondria, Cardiac aging

Background

Aging is a physiological stage accompanied by the functional decline of multiple organs, including the heart. Aging also significantly increases the prevalence of cardiovascular diseases (CVDs) [1]. Heart function, especially diastolic function, declines progressively with age, and this baseline functional decline is accompanied by increased risks of pathological myocardial remodeling, cardiac hypertrophy, arrhythmia, microcirculatory dysfunction, and heart failure (HF) [2]. Due to the high energetic demand of the heart, heart function is tightly regulated by energy metabolism. Compromised mitochondrial structure, bioenergetics, and signaling have been observed in the aging heart [3]. Multiple mechanisms, including increased oxidative stress, mutations in mitochondrial DNA, and dysregulation of proteostasis, have been shown to contribute to age-related mitochondrial dysfunction in the heart [4].

The mammalian mitochondrial proteome consists of more than 1000 different proteins [5]. Mitochondrial proteins can undergo post-translational modifications (PTMs) such as phosphorylation, acetylation, and oxidation. These PTMs add an additional layer of complexity to the mitochondrial proteome and modulate the properties and functions of mitochondrial proteins. PTMs of mitochondrial proteins can regulate intra-cellular signaling, mitochondrial energy generation, apoptosis, autophagy, and response to injury [6, 7]. Protein phosphorylation is one of the most studied PTMs, and deregulated phosphorylation has been implicated in aging and diseases. For example, phosphorylation of cyclophilin D, a regulator of the mitochondrial permeability transition pore (mPTP), has been shown to sensitize mPTP opening and cell death after myocardial ischemia-reperfusion [8]. Nicotinamide adenine dinucleotide (NAD^+) serves as a substrate for protein deacetylation by sirtuins (SIRTs). Cellular NAD^+ levels decline with age [9, 10] and this decline plays a critical role in aging and age-related diseases [10–13]. Compared to young hearts, older hearts have decreased NAD^+ levels and increased levels of total protein acetylation [14]. SIRT3 is the main protein deacetylase within the mitochondria and plays a key regulatory role in mitochondrial metabolism and signaling via protein deacetylation [7, 15]. Besides acetylation, SIRT5 has been shown to catalyze other NAD^+-dependent lysine acyl modifications (i.e., malonylation, succinylation, and glutarylation) in the mitochondria [16]. The changes and functional roles of these PTMs in cardiac aging remain to be established.

Increased mitochondrial oxidative stress is a hallmark of cardiac aging and excess reactive oxygen species (ROS) promotes oxidative modifications on mitochondrial proteins [3]. Redox-related protein modifications like S-oxidation (sulfenylation and sulfinylation), S-nitrosylation, and S-glutathionylation have been shown to contribute to mitochondrial dysfunction in cardiomyocytes during cardiac aging [1, 17, 18]. However, further investigations are needed to expand our understanding of the roles of oxidative PTMs of specific mitochondrial proteins in cardiac aging.

Bottom-up proteomics is a powerful tool used to characterize and quantify differential protein expression as a result of disease, pharmaceutical treatment, environmental changes, phenotypic differences, etc. Bottom-up proteomics methods have even been applied to observe changes in PTMs, primarily by implementing PTM-specific enrichment techniques or protein purification [1, 19]. However, since protein digestion is required for bottom-up methods, information relevant to the intact protein and proteoforms may be lost [20]. For example, bottom-up techniques may not be able to characterize the coordination in PTM motifs, thus limiting their ability to quantify the stoichiometry among different intact proteoforms. On the other hand, top-down mass spectrometry has been introduced as a comprehensive approach to directly measure and quantify intact proteoforms with PTMs [21–25].

As top-down proteomics methods analyze the intact protein directly, the method is ideal for observing changes in proteoform expression with variable PTM motifs. However, a primary challenge in top-down proteomics is the characterization and quantification of proteoforms in complex systems with high dynamic range [26]. This is particularly challenging for mitochondria; these organelles are characterized by having many protein complexes with low abundance from subpopulations found in the mitochondrial membrane [27–30]. Even still, the Ge group has successfully studied heart tissue and cardiac aging using top-down proteomics and identified proteins related to mitochondrial function [31]. Top-down proteomics has also been used to analyze intact

proteins from enriched mitochondria from cultured cells [29, 32, 33].

In this study, we successfully isolated intact mitochondrial proteins from the mouse heart and applied a label-free quantitative top-down proteomics platform to investigate age-related proteoform expression changes. This platform features ultrahigh-pressure liquid chromatography (UPLC)-MS and label-free quantitation, enabling sensitive and high-throughput characterization of proteins. We have applied this platform for comprehensive quantitation of proteoforms expressed in mitochondria collected from young (4 months) and old (24–25 months) mice. In total, we characterized 823 proteoforms from 134 proteins. 20 proteoforms were differentially expressed between the young and old hearts. Among them, 13 proteoforms were decreased in abundance and 7 proteoforms were increased in abundance in the old mice This integrated platform is ideal for characterizing and quantifying intact proteoforms in complex biological samples including difficult-to-study systems such as the mitochondrial proteome.

Methods

Chemicals and Materials. Pierce™ BCA protein assay kit, Halt™ Protease Inhibitor Cocktail 100X, Halt™ Phosphatase Inhibitor Cocktail, tris(2-carboxyethyl) phosphine hydrochloride (TCEP), and n-dodecyl β-D-maltoside (DDM) were obtained from Thermo Fisher (Waltham, MA). Fetal bovine serum was obtained from Fisher Bioreagents. LC-MS grade 2-propanol, acetonitrile, water, trifluoroacetic acid, sucrose, HEPES, EDTA, trypsin (TG522), trypsin inhibitor (T9201), and other chemicals were purchased from Sigma-Aldrich (St. Louis, MO) unless noted otherwise.

Animals. Male C57Bl6 mice were group-housed and maintained on a 14-h light/ dark cycle. The mice in the young group were 4 months old and the mice in the old group were 24–25 months old. Three mice per age group were used for the study. For sample collection, mice were anesthetized with isoflurane and the hearts were excised for mitochondria isolation. All animal procedures were performed based on the Guide for the Care and Use of Laboratory Animals and were approved by the Oklahoma Medical Research Foundation Animal Care and Use Committee.

Cardiac mitochondrial isolation. Mitochondria were isolated using mild trypsin digestion followed by differential centrifugation [34]. Briefly, fresh whole tissue from a single heart was washed and minced in ice-cold isolation buffer (0.3 M sucrose, 10 mM sodium HEPES, pH 7.2, and 0.2 mM EDTA). The tissue was subjected to mild trypsin digestion (1.25 mg) for 10 min at 4 °C and then diluted with an isolation medium (pH 7.4) containing 0.1% BSA and 2.5 mg of trypsin inhibitor. Tissue was homogenized using 4 strokes of a glass/Teflon potter and drill, set to 300 rpm, in 5x tissue volume of complete homogenization buffer (0.3 M sucrose, 10 mM sodium HEPES, pH 7.2, and 0.2 mM EDTA, 0.1% BSA). The homogenate was centrifuged for 10 min at 800 *g* (4 °C). The supernatant solution was decanted and centrifuged for 10 min at 8,000 *g* (4 °C). The supernatant was discarded, and the pellet was twice resuspended in isolation medium then centrifuged for 10 min at 8,000 *g* each time (4 °C). The final pellet corresponds to the mitochondrial fraction of the cardiac cells from the whole heart. The final washed pellet was re-suspended in an isolation buffer with Halt™ Protease Inhibitor (1X), Halt™ phosphatase inhibitor (1X), trichostatin (0.1μM), and nicotinamide (1μM). Protein concentration was determined by bicinchoninic acid assay (BCA). Isolated mitochondria were snap-frozen in liquid nitrogen and stored at −80 °C until use.

Lysis of the mitochondria. The isolated mitochondria from three young and three old mice were resuspended in lysis buffer (20 mM HEPES, 150 mM KCl, 10 mM $MgCl_2$, 1 μM PMSF, 0.05% DDM, pH 7.5) and lysed using sonication. The mitochondrial lysate was then centrifuged at 10,000 rpm for 30 min at 4 °C, and the supernatant was collected.

Denaturation, reduction, and alkylation of intact mitochondrial protein. To the mitochondrial lysate, an equal volume of 8 M urea was added so that the final urea concentration was 3 M. After denaturation, the proteins in the lysate were reduced by adding 0.5 M TCEP and incubated at room temperature for 15 min. The proteins were alkylated by adding 375 mM iodoacetamide (IAA) (final concentration ~ 20 mM). This solution was incubated at room temperature in the dark for 30 min. The denatured, reduced, and alkylated mitochondrial lysate was subjected to ultracentrifugation at 40,000 rpm for 1 h, and the supernatant was collected. The protein concentration was determined using the Pierce™ BCA protein assay kit. Lysate was stored at -80 °C until analysis.

Top-down LC-MS/MS Analysis. To optimize MS conditions, we performed 9 test runs. Then we performed 12 quantitative runs arising from 3 biological replicates in two conditions (young vs. old), with technical duplicates for each sample. A modified Thermo Scientific (Waltham, MA) Accela LC system was used for all the runs [6, 7]. 5 μg of the protein from each sample was loaded onto a home-packed C5 trapping column (150 μm i.d., 5 cm length, Jupiter particles, 5 μm diameter, 300 Å pore size) and then separated using a C4 RPLC Capillary column (100 μm i.d., 60 cm length, 3.4 μm diameter, 300 Å pore size) with a flow rate of 200 nL/min. The composition of mobile phase A (MPA) was 0.01% TFA, 0.585% acetic acid, 2.5% 2-propanol, and 5% acetonitrile in water, and that of mobile phase B (MPB) was 0.01% TFA, 0.585%

acetic acid, 45% 2-propanol, and 45% acetonitrile in water. Orbitrap Exploris 240 mass spectrometer (Thermo Fisher Scientific, Bremen, Germany) with a customized nano-ESI interface was used to analyze the LC eluent. A 100-min gradient from 10 to 70% of MPB was applied. MS parameters were set as follows: inlet capillary temperature was 275 °C, spray voltage was 3.0 kV, and resolution for MS1 and MS2 was set to 120,000 and 60,000 respectively, AGC target was 1×10^6 with 2 micro scans for MS1 and 4 micro scans for MS2. Maximum injection time was 500 ms for MS1 and 300 ms for MS2 scans. The isolation window was set as 2 m/z, the dynamic exclusion window was 90 s, and the top six most abundant precursor ion peaks (charge 4–50) from each MS1 scan were selected for MS2 fragmentation with 35% as normalized higher energy collision dissociation (HCD) energy.

Data Analysis. The results of these 21 runs (9 test runs and 12 quantitative runs) were used to create a proteoform identification library (Supplementary Table 1). TopPIC Suite (version 1.4.10) [35] was used to identify the proteoforms and searched against the annotated *Mus Musculus* database (Uniprot 2023-03-24, 17141 species). For TopPIC, decoy database searching was used with a maximum number of mass shifts set as 2, the FDR cutoff was set as 0.01 for both spectrum and proteoform levels, and the alkylation on cysteine residues was used as a fixed modification. All other parameters were set as default. The identification library was generated by combining all the identified proteoforms from all datasets. ProSight Lite was used for manual interpretation and spectrum presentation [36].

The collected top-down datasets were deconvoluted and quantified using Biopharma Finder (Thermo Fisher Scientific). An in-house Python software was written for label-free quantitation. This software utilizes an accurate mass and time (AMT) approach to merge mass features between runs [24, 37]. The mass features from different runs were combined and filtered with ±10 ppm mass shift and ±5 min retention time shift. The proteoform library was merged with the quantified mass features. The reported results were confirmed with manual evaluation. The mass spectrometry proteomics data have been deposited to the ProteomeXchange Consortium via the PRIDE [38] partner repository with the dataset identifier PXD051505.

Results

Identification of intact mitochondrial proteoforms in young and old mice. The experimental design for the top-down proteomic analysis of intact mitochondrial proteins is shown in Fig. 1. Intact protein lysate was extracted from purified mitochondria of 3 young (4 months) and 3 old (24–25 months) mice [34]. 5 µg of the extracted mitochondrial proteins were analyzed using LC-MS/MS in technical duplicate. TopPIC Suite was used for protein identification.

In total, we identified 823 unique proteoforms of 134 unique mitochondrial proteins (Supplementary Table 1). These proteoforms ranged in size from ~3 kDa to nearly 35 kDa (Fig. 2A). These proteoforms demonstrated a diverse set of PTMs, including acetylation (*N*-terminal acetylation and lysine acetylation), succinylation, oxidation, and phosphorylation (Fig. 2C). Many proteoforms carry unknown modifications, either from a combination of multiple PTMs that cannot be distinguished by the MS/MS or from novel PTMs that have not been well-studied. Approximately half of the proteins were expressed as only one proteoform; however, many proteins were expressed as multiple proteoforms (Fig. 2B and Supplementary Table 1) and, impressively, one protein, the electron transfer protein subunit beta (ETFB, Q9DCW4) had more than 140 characterized proteoforms. We characterized the intact proteoform that underwent endogenous *N*-terminal methionine removal and acetylation at the N-terminal alanine. Out of the total 144 proteoforms that were studied, approximately 76% of them were found to be PTM-modified proteoforms. However, many of them had uncharacterized mass shifts, which suggests either a combination of various PTMs or unknown PTMs. The remaining 58 proteoforms characterized here were found to be truncated.

Further, we used Mito Carta 3.0 and UniProt to determine if the proteins are localized in the mitochondria and categorize the sub-organelle localization of the identified mitochondrial proteins, Fig. 2D**&**E [5]. Most identified proteins are localized in the mitochondria (96 out of 134 proteins; 72%) and a majority of them (52 proteins out of 96 mitochondrial proteins) are localized in the inner mitochondrial membrane (IMM). Of these, 28 of the identified proteins are components of the oxidative phosphorylation (OXPHOS) complexes. These OXPHOS proteins include subunits from all five complexes (Complex I-V). The second largest sub-organelle class of identified proteins consist of those located in the mitochondrial matrix. This class includes a small group of matrix proteins involved in the TCA cycle. In addition, 4 proteins located in the intermembrane space (IMS) and 3 proteins located in the outer mitochondrial membrane (OMM) were also identified.

Quantitative comparison of intact mitochondrial proteoforms in young and old hearts. Biopharma Finder (ThermoFisher Scientific) was used to deconvolute and quantify the identified mass features. Student's *t*-tests were used to determine the statistical significance of the fold change of each proteoform between the young and old hearts [39]. To be considered statistically significant the p-value should be less than 0.05 (95% confidence).

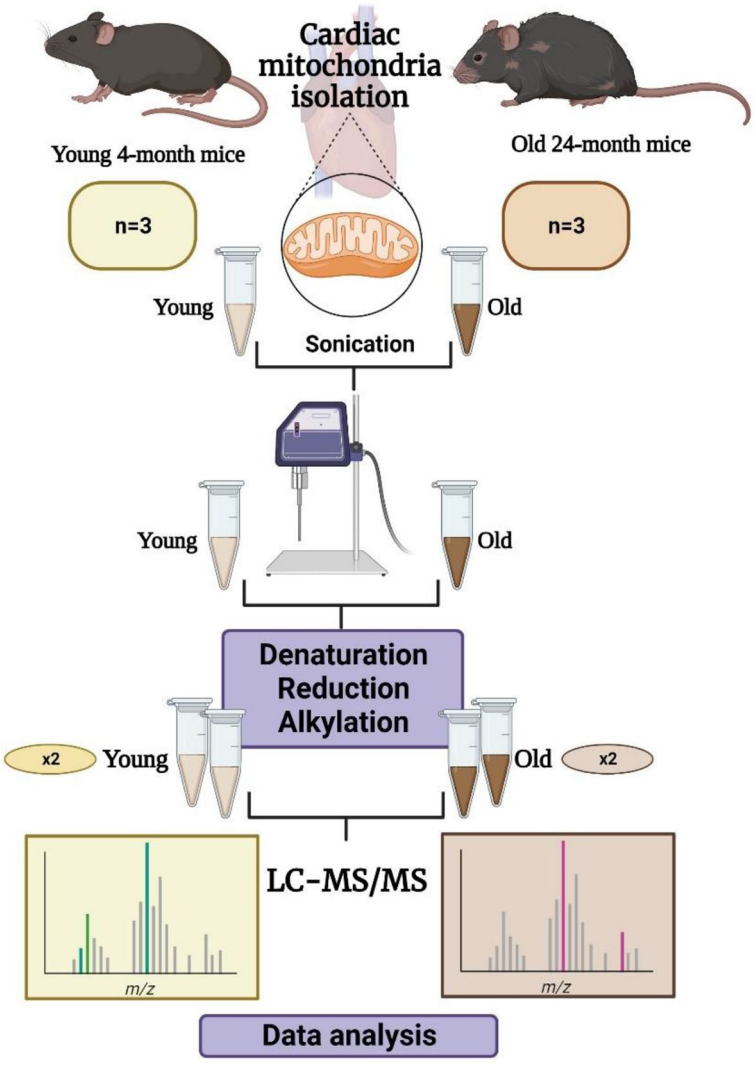

Fig. 1 Schematic for intact mitochondrial proteome profiling using quantitative top-down proteomics

Fold change was calculated using the ratio of average intensities of the mass features in both conditions.

A volcano plot was created to visualize the differential expression of proteoforms between young and old hearts (Fig. 3A). Overall, 20 proteoforms were differentially expressed between the young and old hearts. Thirteen (13) proteoforms were decreased in abundance and 7 proteoforms were increased in abundance in the old mice (Supplementary Table 2). For example, the expression of NADH dehydrogenase [ubiquinone] iron-sulfur protein 6 (NDUS6; P52503), an accessory subunit of Complex I, was significantly reduced in old hearts compared to young hearts (Fig. 3B). Other mitochondrial proteins that had identified proteoforms with decreased abundance in cardiac mitochondria from the old mouse group included cytochrome c oxidase subunit 6B1 (CX6B1, P56391), NADH dehydrogenase [ubiquinone] flavoprotein 3 (NDUV3, Q8BK30), glutaredoxin-related protein 5 (GLRX5, Q80Y14), cytochrome b-c1 complex subunit 6 (QCR6, P99028). Other proteins that increased in abundance in the old mouse samples included mitochondrial import inner membrane translocase subunit Tim8 A (Tim8A, Q9WVA2), cytochrome c, somatic (CYC, P62897), electron transfer flavoprotein subunit beta (ETFB, Q9DCW4), and malate dehydrogenase (MDHM, P08249).

In addition to changes in protein abundance, we have investigated PTM-specific changes with aging. For instance, we identified 3 different proteoforms of NADH dehydrogenase ubiquinone 1 alpha subcomplex subunit 2 (NDUA2, Q9CQ75). The most abundant proteoform was acetylated at the *N*-terminal (Fig. 4A). Another proteoform was expressed at lower abundance and was acetylated at the N-terminal and oxidized at Met-90 (*data not shown*). This proteoform was present at very low intensity and was not quantifiable in this dataset. Oxidation of

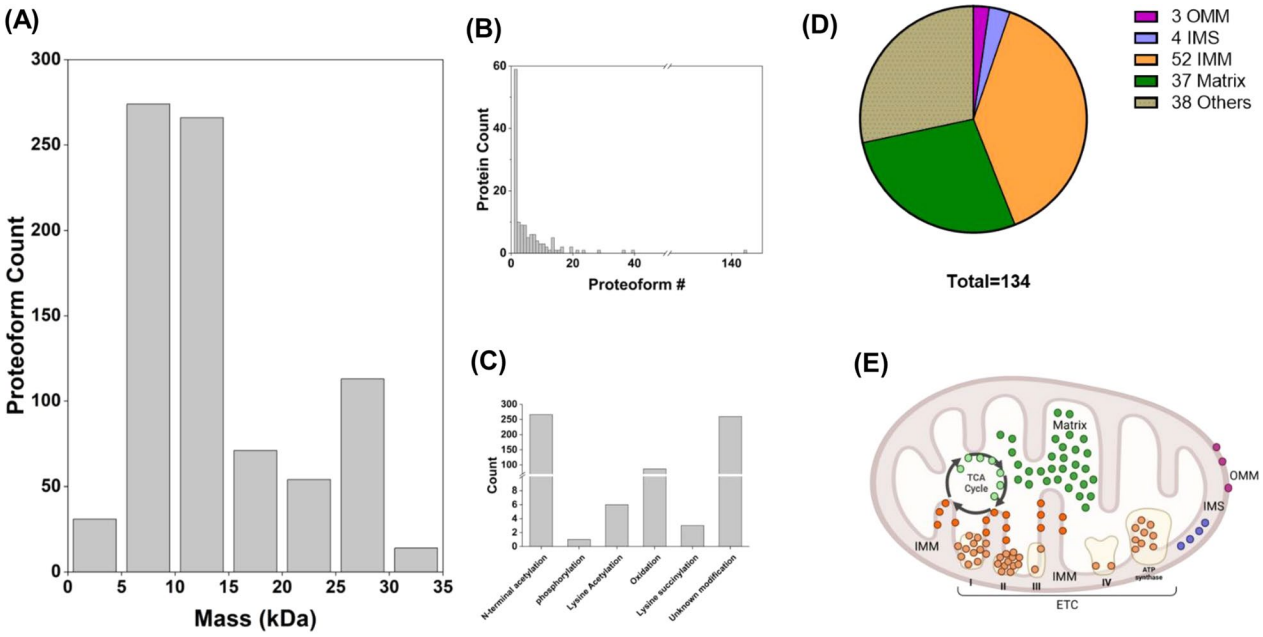

Fig. 2 Identification of intact proteoforms from enriched cardiac mitochondria. (**A**) Histogram demonstrating the mass distribution of uniquely identified proteoforms; (**B**) Bar graph demonstrating the number of unique proteoforms identified per protein; (**C**) Bar graph depicting the number of PTMs identified; (**D**) Pie chart demonstrating the location of the identified proteins in the mitochondria and intercellular space; (**E**) Visualization of the identified protein in the mitochondria

intact proteoforms can be endogenous or artificial, however, in this case, the abundance of the oxidized proteoform is negligible. The remaining identified proteoform was acetylated at the *N*-terminal (Fig. 4B), oxidized at Met-90, and succinylated at Lys-97. No intact proteoforms were detected that were only succinylated at Lys-97 with no oxidation at Met-90. Both the *N*-terminally acetylated proteoform and the oxidized and succinylated proteoform showed a decreasing abundance trend in the old mice, although this change in expression was only significant for the succinylated and oxidized proteoform, Fig. 4C. Interestingly, the ratio of the oxidized and succinylated proteoform compared with the *N*-terminally acetylated proteoform was shown to significantly increase in the old mice, Fig. 4D. This protein has been previously reported to be succinylated at Lys-64 [40]; however, our results show that lysine residue 97 can also be succinylated.

Three proteoforms of the 10 kDa Heat Shock protein, mitochondrial (CH10, Q64433) were identified. One proteoform was acetylated at the *N*-terminal (Fig. 5A), the second proteoform maintained *N*-terminal acetylation and was also oxidized at Met-31 (Fig. 5B), and the third proteoform maintained the previously mentioned modifications and was also acetylated at Lys-39 (Fig. 5C). This lysine has previously been reported to be acetylated in the Uniprot database [41]. Overall, the expression of all three proteoforms for this protein trended down in the old mice, although only the second and the third proteoforms were significantly decreased (Fig. 5D). Interestingly, when the ratio of these two proteoforms normalized to the *N*-terminally acetylated proteoform was examined, we found that the ratio of these two proteoforms did not decrease (Fig. 5D).

These two examples show that changes in stoichiometry in different PTM-modified intact proteoforms may not be reflected by the expression of a single proteoform or a single peptide. On the other hand, these changes, even for proteoforms with combinatorial PTMs, can be readily observed for intact proteoforms analyzed using top-down proteomics. This, however, may not be possible using bottom-up proteomics data.

Discussion

Aging is a major risk factor for the development of cardiac disease. The heart is a highly metabolic organ and its proper functioning is highly dependent on healthy mitochondria to supply sufficient energy [42]. The study of age-related mitochondrial changes has been an important research field for many years; however, the dynamic range in protein abundance of mitochondrial proteins has made it difficult to study intact proteoforms with PTMs that may be related to metabolic function. Bottom-up proteomics techniques are sensitive and robust and can be used for the high-throughput, quantitative study of complex biological systems including mitochondrial proteins [43, 44]. However, bottom-up proteomics methods require protein digestion which can obscure

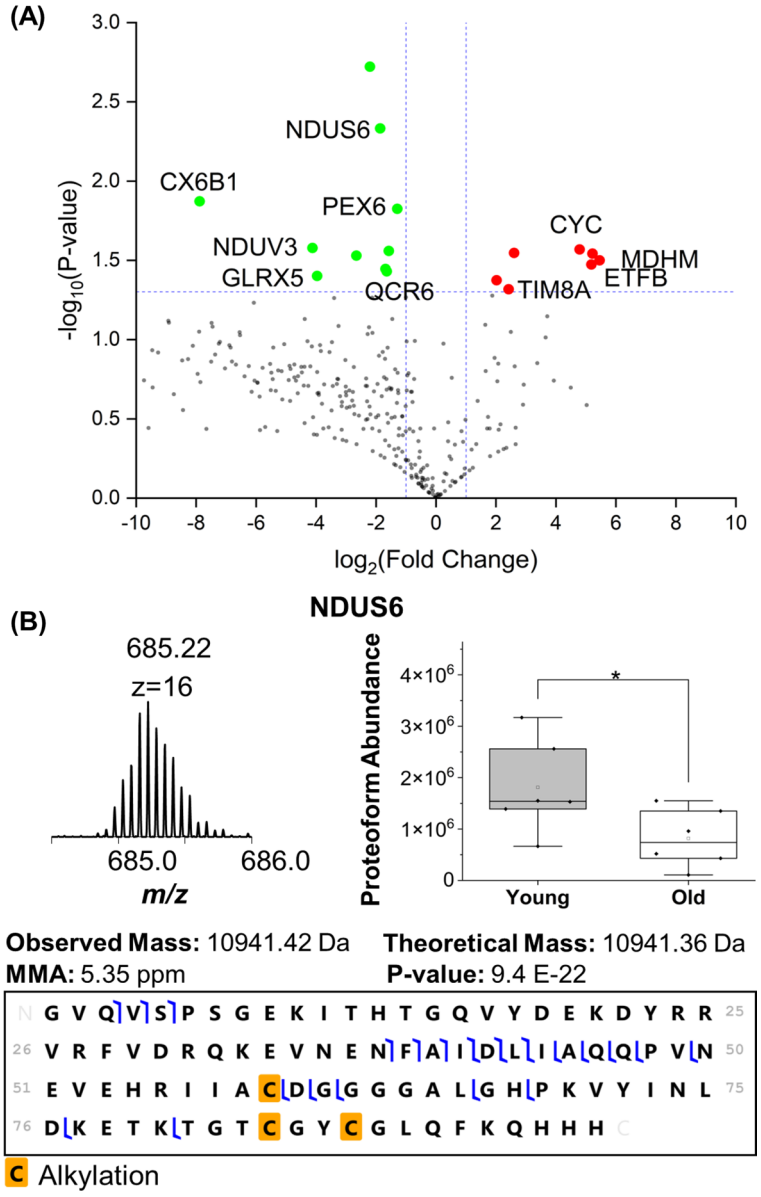

Fig. 3 Examination of the change in intact mitochondrial proteoform abundance as a function of age. (**A**) Volcano plot demonstrating the differential expression of identified proteoforms. The vertical dotted lines represent a log2 fold change cutoff of 1, and the horizontal dotted line represents a – log10 p-value cutoff of 1.3. The proteoforms that were increased in the old mouse samples are shown in red and the decreased proteoforms are shown in green. (**B**) Expression of NADH dehydrogenase [ubiquinone] iron-sulfur protein 6 (NDUS6; P52503) was found to be significantly reduced in old mitochondria samples

important information regarding the intact proteoforms including PTM motifs and other modifications [22, 45].

Top-down proteomics analyzes the intact proteoforms directly so information regarding protein modifications is maintained. However, previous applications of top-down proteomics to complex biological systems have been challenging due to the relatively low sensitivity of the methods and the high dynamic range of the samples. Improvements to liquid chromatography [21, 46–48] and mass spectrometry [49] methods concerning separation efficiency and sensitivity have allowed the application of top-down proteomics to important biological systems such as age-related systems. These new applications can give us new insight into the pathophysiological mechanisms of age-related cardiovascular disease [50, 51]. Using our developed label-free quantitative top-down proteomics UPLC-MS/MS platform [52], we have studied, for the first time, age-related differential expression of mitochondrial proteoforms extracted from enriched cardiac mitochondria in mice.

In this survey study, we identified a total of 134 proteins in the samples and 96 of them (72%) were mitochondrial

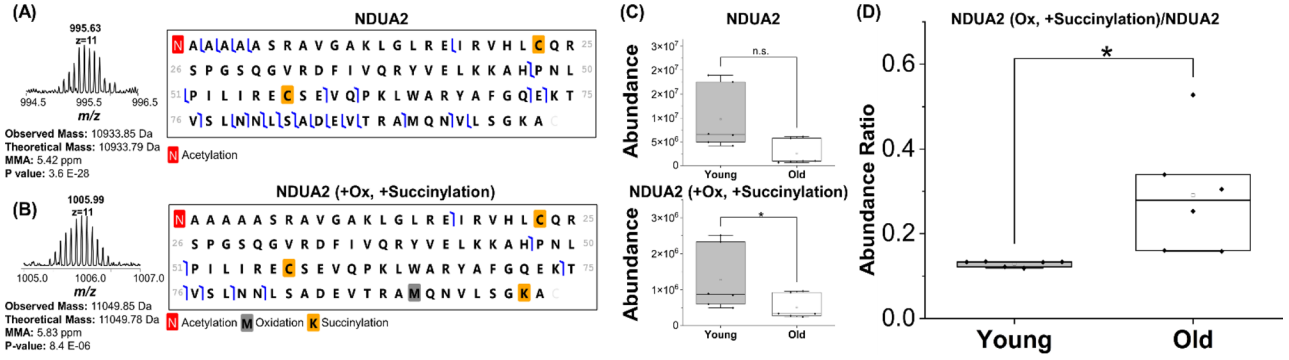

Fig. 4 Quantitative analysis of the NADH dehydrogenase 1 alpha subcomplex subunit 2 (NDUA2, Q9CQ75) protein. (**A**-**B**) Isotopic distribution and fragment map of the identified proteoforms. (**C**) Box and whisker plots demonstrating the abundance of each proteoform in young and old mouse samples. (**C**) The ratio between different proteoforms in young and old mouse samples

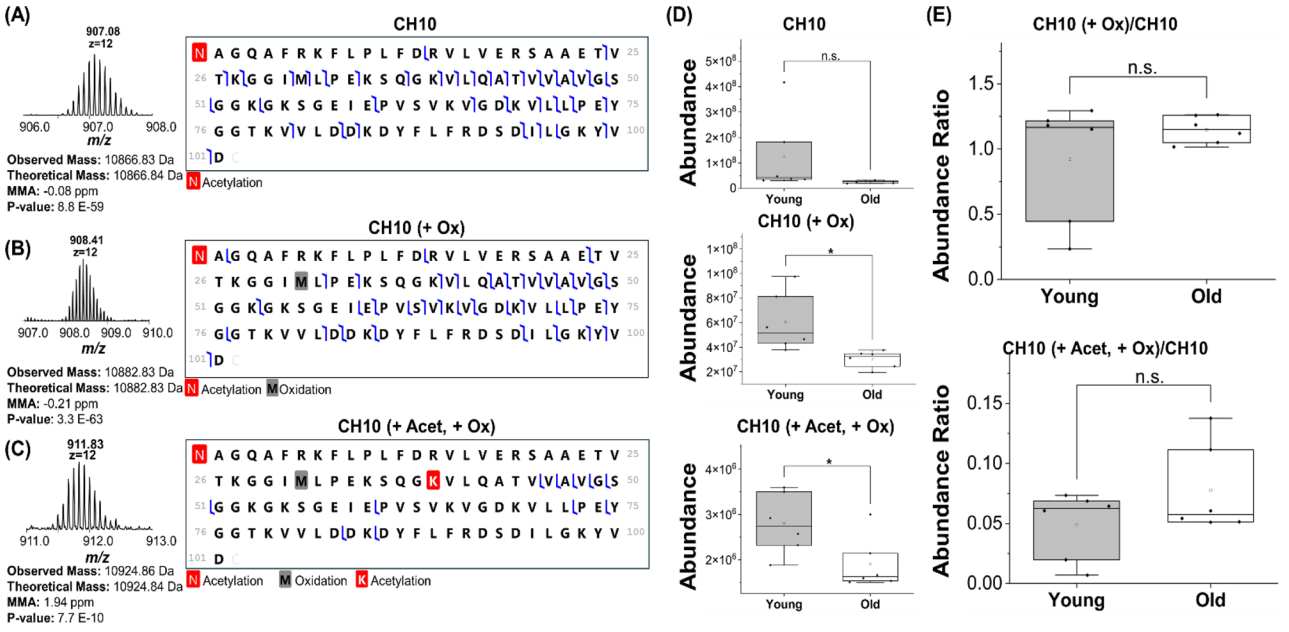

Fig. 5 Quantitative analysis of the 10 kDa Heat shock protein (CH10, Q64433) protein. (**A**-**B**) Isotopic distribution and fragment map of the identified proteoforms. (**C**) Box and whisker plots demonstrating the abundance of each proteoform in young and old mouse samples. (**D**) The ratio between different proteoforms in young and old mouse samples

proteins (Fig. 2D). This result validated the successful enrichment of mitochondrial proteins by our mitochondrial isolation method and demonstrated the compatibility of the enrichment method with top-down proteomics analysis. Moreover, we identified mitochondrial proteins located in all sub-mitochondrial compartments (OMM, IMS, IMM, matrix), supporting that intact mitochondria were isolated. Proteins located in the IMM comprise over 50% of the mitochondrial proteins identified. Among the 52 IMM proteins were detected, 28 of them are OXPHOS proteins. This high percentage is consistent with the high abundances of OXPHOS proteins which represent two-thirds of the total proteins of the IMM. On the other hand, we detected a low number of proteins located in the IMS and OMM. The lower number of proteins detected in these sub-mitochondrial compartments is consistent with the lower numbers of proteins present in these compartments. Specifically, OMM proteins account for approximately 10% of all mitochondrial proteins, and IMS proteins represent about 5% of all mitochondrial proteins [5].

Using label-free quantitative top-down proteomics, we detected age-related changes in the abundance of intact proteoforms in heart mitochondria (Fig. 3A). Four proteins (NDUS6, NDUV3, CX6B1, and OCR6) that exhibited reduced abundance with aging are subunits of the ETC complex, and our result is consistent with previous findings on aging-associated decline in energy metabolism and reduced expression of genes coding for oxidative phosphorylation mitochondrial proteins [53, 54]. The

lower levels of ETC complex subunits may contribute to reduced ATP production and impaired bioenergetics of the heart with aging. Another protein with reduced expression with aging is glutaredoxin 5 (GLRX5), a mitochondrial glutaredoxin involved in iron/sulfur protein assembly [55]. Iron/sulfur clusters mediate electron transfer in complex I, II and III of the ETC, which are also major sites of mitochondrial ROS production [56]. Thus, reduced GLRX5 expression may inhibit electron transfer in ETC and increase mitochondrial ROS production. GLRX5 has been shown to protect against oxidative stress in yeast and osteoblasts [57, 58]. The reduced expression of GLRX5 in old hearts may in part contribute to the increase in mitochondrial oxidative stress in the aging heart [3].

For proteins that were detected with increased abundance with aging, TIM8A is a small Tim chaperone protein involved in the assembly of Complex IV [59]. A previous study has shown that TIM8A expression decreases when a GSK inhibitor induces cardioprotection [60]. Whether increased TIM8A contributes to cardiac dysfunction in the aging heart remains to be investigated. We also detected an age-related increase in the level of ETFB, a flavoprotein involved in mitochondrial metabolism. ETFB is associated with anthracycline-mediated mitochondrial dysfunction in cardiotoxicity in cancer patients but its role in mitochondrial dysfunction in cardiac aging is unclear [61].

Cardiac proteins are continuously synthesized and degraded to ensure protein homeostasis. In addition to dynamic changes in protein expression, PTMs of proteins offer another regulatory mechanism to fine-tune protein function and in turn, modulate different cellular processes. PTMs of proteins can regulate protein folding, half-life of proteins, and protein-protein interactions [62]. Multiple post-translational modifying enzymes have been identified in the mitochondria, and several PTMs have been described in mitochondria [63].

In this study, we detected three main PTMs, oxidation, acetylation, and succinylation, in cardiac mitochondrial proteins. Increased protein oxidation due to high ROS production is an age hallmark of cardiac aging and contributes to the dysregulation of mitochondrial dynamics and protein quality control [64]. Lysine acetylation and succinylation are two forms of protein acylation modifications. Mitochondrial protein acetylation and succinylation can be removed by NAD^+-dependent deacetylases sirtuins SIRT3 and SIRT5 [65, 66]. NAD^+ depletion, reduced SIRT3 and SIRT5 activity and increased lysine acylation have been implicated as pathogenic mechanisms in **CVDs** [67, 68]. The quantitative top-down proteomics platform developed here quantifies changes in PTMs of intact mitochondrial proteoforms and allows us to study combinatorial changes in these PTMs. This allows the observation of changes to proteoform-level expression and characterization of the physiologically active proteoforms. For example, two proteoforms of the NDUA2 protein were identified (Fig. 4A). One proteoform underwent N-terminal methionine removal and acetylation of the N-terminal alanine and the other proteoform maintained the N-terminal methionine cleavage in addition to succinylation and oxidation at Lys-97 and Met-90, respectively. A third proteoform was identified that demonstrated N-terminal methionine cleavage and oxidation at Met-90 was observed with low intensity and the succinylated proteoform without oxidation was not observed. This indicates that oxidation at Met-90 and succinylation at Lys-97 may be combinatorial, which is challenging to determine using bottom-up proteomics methods that require digestion and may obscure the connectivity between the PTMs. Furthermore, there was no significant change in the abundance of the absolute levels of the proteoform with only N-terminal methionine removal and acetylation at the N-terminal alanine residue in NDUA2 in young and old hearts, but there was a significant decrease in the abundance of the succinylated/oxidized proteoform. Our top-down method, however, allowed us to observe an increased ratio of succinylated/un-succinylated NDUA2 proteoforms, suggesting increased succinylation of NDUA2 with aging (Fig. 4C and D). This result highlights the importance of normalization to the level of the un-modified proteoform when investigating the change in a specific PTM. NDUA2 is an accessory subunit of complex I and may be involved in regulating the assembly or activity of complex I. Increased succinylation of NDUA2 could potentially impair complex assembly and activity in the aging heart.

Despite the enrichment of mitochondrial proteins, we still detected proteins located in other subcellular compartments, suggesting the presence of non-mitochondrial contaminants such as peroxisomes, ER, and Golgi [69]. LC-MS/MS is a sensitive technique that can detect small amounts of contaminating proteins. Physical interaction between mitochondria and these organelles makes the purification process challenging; complementing differential centrifugation with another separation technique could enhance the purity of the mitochondrial fraction [70, 71].

In this study, intact mitochondrial proteoforms were extracted using an aqueous buffer, omitting any detergent to solubilize insoluble hydrophobic proteins such as membrane proteins. As the structure of mitochondria involves a complex membrane system with many membrane-bound proteins, a biological limitation of this technique is the inability to characterize insoluble membrane proteins. Previous studies have analyzed intact mitochondrial membrane proteins from cultured cells [33]. Recently, there have been reports of MS-compatible

detergents for top-down proteomics analysis of insoluble proteins [72, 73]. Future application of these MS-compatible detergents could allow top-down proteomics analysis of intact proteoforms from mitochondria enriched from tissue.

Further improvements regarding intact protein separation efficiency, quantitation, and MS sensitivity could improve proteoform characterization and quantitation for this method. For example, other separation techniques such as capillary electrophoresis that have higher sensitivity and separation efficiency compared with LC methods have been implemented for top-down proteomics [74–77]. Additionally, multidimensional separation of intact proteins has been shown to improve separation efficiency and allow for the characterization of more intact proteoforms in complex samples [21, 78–84]. However, label-free quantitation techniques as used here are challenging to implement with multidimensional separation methods. The application of isobaric chemical tag labeling would allow proteoform quantitation in multidimensional separations [22]. Fortunately, recent reports have demonstrated the development of isobaric chemical tag labeling methods for intact proteins [30, 85–90], and coupling these techniques could greatly improve quantitative top-down proteomics methods. Finally, high-field asymmetric waveform ion mobility spectrometry (FAIMS) methods have been applied for intact protein MS analysis to reduce noise and improve the signal-to-noise ratio [76, 77].

Overall, we have demonstrated the benefits of a quantitative top-down proteomics platform to study intact mitochondrial proteoforms enriched from tissue. We identified and quantified hundreds of intact mitochondrial proteoforms for deep characterization of the mitochondrial phenotype for the hearts of young and old mice. While the scope of this initial study was somewhat limited by the relatively small sample size (e.g., 3 young mice and 3 old mice), the platform developed here can facilitate future comprehensive discovery proteomics studies of the intact mitochondrial proteome with improved statistical power. These large-scale studies can lead to the discovery of proteoforms of interest that can be targeted for more precise characterization and localization of PTMs. Additionally, these comprehensive proteomics studies can be integrated with current bottom-up proteomics methodologies to improve PTM localization and proteoform characterization.

Conclusion

Altogether, we have shown the potential of quantitative top-down proteomics techniques to identify and quantify, for the first time, age-related changes in mitochondrial proteoforms directly from enriched mitochondria from the heart. Analysis of proteoforms in mitochondria samples has traditionally been difficult because of low proteoform abundance and high dynamic range; however, with our enrichment strategy of subcellular fractionation coupled with our ultrahigh-pressure separation coupled with sensitive MS detection, we identified hundreds of intact proteoforms from more than 100 proteins from different sub-mitochondrial compartments. In addition to identifying age-related changes in protein abundance, our top-down proteomic analysis provides a bird's eye view of combinatorial PTMs in intact mitochondrial proteoforms. Overall, this survey study demonstrates the capabilities of intact mitochondrial proteoform characterization and quantification by enriching mitochondria from cardiac tissue followed by highly sensitive UPLC-MS/MS analysis.

Supplementary Information

The online version contains supplementary material available at https://doi.org/10.1186/s12014-024-09509-1.

Supplementary Material 1

Supplementary Material 2

Author contributions

ARS and ATS: Conceptualization, Investigation, Visualization, Writing—Original draft preparation; KC-S: Visualization, Writing—Original draft preparation, Supporting—Investigation,; TC and ZZ: Supporting—Visualization; SW and YAC: Supervision, Conceptualization, Writing—Reviewing and Editing, Funding acquisition.

Funding

This work was partly supported by grants from OCAST HR23-169 (SW), NIH NIAID R01AI141625 (SW), NIH NIH/NIAID2U19AI062629 (SW), and Glenn Foundation and/AFAR Ggrant for Junior Faculty (YAC). SW would like to thank the University of Alabama for the support received from the startup fund.

Data availability

No datasets were generated or analysed during the current study.

Declarations

Competing interests

The authors declare no competing interests.

Author details

[1]Aging and Metabolism Research Program, Oklahoma Medical Research Foundation, MS21, 825 NE 13th St, Oklahoma City, OK 73104, USA
[2]Department of Chemistry and Biochemistry, University of Alabama, 250 Hackberry ln, Tuscaloosa, AL 35487, USA
[3]Department of Chemistry and Biochemistry, University of Oklahoma, 101 Stephenson Parkway, Room 2210, Norman, OK 73019-5251, USA

Received: 16 January 2024 / Accepted: 19 September 2024
Published online: 30 September 2024

References

1. Yan M et al. *Cardiac Aging: From Basic Research to Therapeutics.* Oxidative Medicine and Cellular Longevity, 2021. 2021: p. 9570325.
2. Xie S, et al. Metabolic landscape in cardiac aging: insights into molecular biology and therapeutic implications. Signal Transduct Target Therapy. 2023;8(1):114.

3. Chiao YA, Rabinovitch PS. The Aging Heart. Cold Spring Harb Perspect Med. 2015;5(9):a025148.
4. Tocchi A, et al. Mitochondrial dysfunction in Cardiac Ageing. Biochim Biophys Acta. 2015;1847(11):1424–33.
5. Rath S, et al. MitoCarta3.0: an updated mitochondrial proteome now with sub-organelle localization and pathway annotations. Nucleic Acids Res. 2021;49(D1):D1541–7.
6. Hofer A, Wenz T. Post-translational modification of mitochondria as a novel mode of regulation. Exp Gerontol. 2014;56:202–20.
7. Stram AR, Payne RM. Posttranslational modifications in Mitochondria: protein signaling in the powerhouse. Cell Mol Life Sci. 2016;73(21):4063–73.
8. Hurst S, et al. Phosphorylation of cyclophilin D at serine 191 regulates mitochondrial permeability transition pore opening and cell death after ischemia-reperfusion. Cell Death Dis. 2020;11(8):661.
9. Braidy N, et al. Age related changes in NAD + metabolism oxidative stress and Sirt1 activity in Wistar rats. PLoS ONE. 2011;6(4):e19194.
10. Tarrago MG, et al. A potent and specific CD38 inhibitor ameliorates Age-related metabolic dysfunction by reversing tissue NAD(+) decline. Cell Metab. 2018;27(5):1081–e109510.
11. Camacho-Pereira J, et al. CD38 dictates age-related NAD decline and mitochondrial dysfunction through an SIRT3-Dependent mechanism. Cell Metab. 2016;23(6):1127–39.
12. Mills KF, et al. Long-term administration of Nicotinamide Mononucleotide mitigates Age-Associated physiological decline in mice. Cell Metab. 2016;24(6):795–806.
13. Zhang H, et al. NAD(+) repletion improves mitochondrial and stem cell function and enhances life span in mice. Science. 2016;352(6292):1436–43.
14. Yeo D, Kang C, Ji LL. Aging alters acetylation status in skeletal and cardiac muscles. Geroscience. 2020;42(3):963–76.
15. Anderson KA, Hirschey MD. Mitochondrial protein acetylation regulates metabolism. Essays Biochem. 2012;52:23–35.
16. Nishida Y, et al. SIRT5 regulates both cytosolic and mitochondrial protein malonylation with Glycolysis as a major target. Mol Cell. 2015;59(2):321–32.
17. Quan Y, et al. Mitochondrial ROS-Modulated mtDNA: a potential target for Cardiac Aging. Oxidative Med Cell Longev. 2020;2020:p9423593.
18. Kornfeld OS, et al. Mitochondrial reactive oxygen species at the heart of the Matter. Circul Res. 2015;116(11):1783–99.
19. Riley NM, Coon JJ. Phosphoproteomics in the age of Rapid and Deep Proteome Profiling. Anal Chem. 2016;88(1):74–94.
20. Chait BT. Mass Spectrometry: Bottom-Up or Top-Down? Science. 2006;314(5796):65–6.
21. Wang Z, et al. Development of an online 2D ultrahigh-pressure Nano-LC system for High-pH and Low-pH reversed phase separation in top-down proteomics. Anal Chem. 2020;92(19):12774–7.
22. Cupp-Sutton KA, Wu S. High-throughput quantitative top-down proteomics. Mol Omics. 2020;16(2):91–9.
23. Pesavento JJ, et al. Shotgun annotation of histone modifications: a New Approach for Streamlined characterization of proteins by Top Down Mass Spectrometry. J Am Chem Soc. 2004;126(11):3386–7.
24. Wu S, et al. Quantitative analysis of human salivary gland-derived intact proteome using top-down mass spectrometry. Proteomics. 2014;14(10):1211–22.
25. Gault J, et al. A combined mass spectrometry strategy for complete post-translational modification mapping of Neisseria meningitidis major pilin. J Mass Spectrom. 2013;48(11):1199–206.
26. Heusch G, et al. Mitochondrial STAT3 activation and cardioprotection by ischemic postconditioning in pigs with regional myocardial ischemia/reperfusion. Circul Res. 2011;109(11):1302–8.
27. Wei L, et al. Novel Sarcopenia-related alterations in Sarcomeric protein post-translational modifications (PTMs) in skeletal muscles identified by top-down proteomics *. Mol Cell Proteom. 2018;17(1):134–45.
28. Seckler HdS, et al. A targeted, Differential Top-Down Proteomic Methodology for comparison of ApoA-I proteoforms in individuals with high and low HDL efflux capacity. J Proteome Res. 2018;17(6):2156–64.
29. Schaffer LV, et al. Identification and quantification of murine mitochondrial proteoforms using an Integrated Top-Down and Intact-Mass Strategy. J Proteome Res. 2018;17(10):3526–36.
30. Yu D, et al. Quantitative top-down proteomics in Complex samples using protein-level Tandem Mass Tag labeling. J Am Soc Mass Spectrom. 2021;32(6):1336–44.
31. Melby JA, et al. High sensitivity top–down proteomics captures single muscle cell heterogeneity in large proteoforms. Proc Natl Acad Sci. 2023;120(19):e2222081120.
32. Catherman AD, et al. Large-scale top-down proteomics of the human proteome: membrane proteins, Mitochondria, and Senescence *. Mol Cell Proteom. 2013;12(12):3465–73.
33. Catherman AD, et al. Top down proteomics of human membrane proteins from enriched mitochondrial fractions. Anal Chem. 2013;85(3):1880–8.
34. Boehm EA, et al. Increased uncoupling proteins and decreased efficiency in palmitate-perfused hyperthyroid rat heart. Am J Physiol Heart Circ Physiol. 2001;280(3):H977–83.
35. Kou Q, et al. TopPIC: a software tool for top-down mass spectrometry-based proteoform identification and characterization. Bioinformatics, 2016;32(22):3495-3497
36. Fellers RT, et al. ProSight Lite: graphical Software to Analyze Top-Down Mass Spectrometry Data. Proteomics. 2015;15(7):1235–8.
37. Paša-Tolić L, et al. Proteomic analyses using an accurate mass and time tag strategy. Biotechniques. 2004;37(4):621–39.
38. Perez-Riverol Y, et al. The PRIDE database resources in 2022: a hub for mass spectrometry-based proteomics evidences. Nucleic Acids Res. 2021;50(D1):D543–52.
39. Lin Z et al. *Simultaneous Quantification of Protein Expression and Modifications by Top-down Targeted Proteomics: A Case of the Sarcomeric Subproteome *^[S]*. Molecular & Cellular Proteomics, 2019. 18(3): pp. 594–605.
40. Park J, et al. SIRT5-Mediated lysine desuccinylation impacts diverse metabolic pathways. Mol Cell. 2013;50(6):919–30.
41. Rardin MJ, et al. Label-free quantitative proteomics of the lysine acetylome in mitochondria identifies substrates of SIRT3 in metabolic pathways. Proc Natl Acad Sci USA. 2013;110(16):6601–6.
42. B M-F., *Mitochondria and oxidative stress in heart aging*. Age. 2016;38(4):225–38.
43. Kiri AN, et al. Proteomic changes in bovine heart mitochondria with age: using a novel technique for organelle separation and enrichment. J Biomol Tech. 2005;16(4):371–9.
44. Zhang Y, et al. Protein analysis by Shotgun/Bottom-up proteomics. Chem Rev. 2013;113(4):2343–94.
45. Toby TK, Fornelli L, Kelleher NL. Progress in Top-Down Proteomics and the analysis of Proteoforms. Annual Rev Anal Chem. 2016;9(1):499–519.
46. Melby JA, et al. Novel strategies to address the challenges in Top-Down Proteomics. J Am Soc Mass Spectrom. 2021;32(6):1278–94.
47. Shen Y, et al. High-resolution ultrahigh-pressure long column reversed-phase liquid chromatography for top-down proteomics. J Chromatogr A. 2017;1498:99–110.
48. Cai W, et al. Top-down proteomics of large proteins up to 223 kDa enabled by serial size Exclusion Chromatography Strategy. Anal Chem. 2017;89(10):5467–75.
49. Yuan H, et al. Recent advances in multidimensional separation for Proteome Analysis. Anal Chem. 2019;91(1):264–76.
50. Cai W, et al. Top-down proteomics: technology advancements and applications to Heart diseases. Expert Rev Proteomics. 2016;13(8):717–30.
51. Gregorich ZR, Chang Y-H, Ge Y. Proteomics in heart failure: top-down or bottom-up? Pflügers Archiv - Eur J Physiol. 2014;466(6):1199–209.
52. Wang Z, et al. Top-down Mass Spectrometry analysis of human serum Autoantibody Antigen-binding fragments. Sci Rep. 2019;9(1):2345.
53. Dai DF, et al. Altered proteome turnover and remodeling by short-term caloric restriction or rapamycin rejuvenate the aging heart. Aging Cell. 2014;13(3):529–39.
54. Emelyanova L, et al. Effect of aging on mitochondrial energetics in the Human Atria. J Gerontol Biol Sci Med Sci. 2018;73(5):608–16.
55. Rodriguez-Manzaneque MT, et al. Grx5 is a mitochondrial glutaredoxin required for the activity of iron/sulfur enzymes. Mol Biol Cell. 2002;13(4):1109–21.
56. Read AD, et al. Mitochondrial iron-sulfur clusters: structure, function, and an emerging role in vascular biology. Redox Biol. 2021;47:102164.
57. Rodriguez-Manzaneque MT, et al. Grx5 glutaredoxin plays a central role in protection against protein oxidative damage in Saccharomyces cerevisiae. Mol Cell Biol. 1999;19(12):8180–90.
58. Linares GR, et al. Glutaredoxin 5 regulates osteoblast apoptosis by protecting against oxidative stress. Bone. 2009;44(5):795–804.
59. Anderson AJ, et al. Human Tim8a, Tim8b and Tim13 are auxiliary assembly factors of mature complex IV. EMBO Rep. 2023;24(8):e56430.
60. Nguyen T, et al. Acute inhibition of GSK causes mitochondrial remodeling. Am J Physiol Heart Circ Physiol. 2012;302(11):H2439–45.

61. Ruiz-Pinto S, et al. Exome array analysis identifies ETFB as a novel susceptibility gene for anthracycline-induced cardiotoxicity in cancer patients. Breast Cancer Res Treat. 2018;167(1):249–56.
62. KA L. Functional decorations: post-translational modifications and heart disease delineated by targeted proteomics. Genome Med, 2013 Feb 28. 5(2).
63. Hofer A. Post-translational modification of mitochondria as a novel mode of regulation. Exp Gerontol. 2014;56:202–20.
64. Chiao YA, et al. Late-life restoration of mitochondrial function reverses cardiac dysfunction in old mice. Elife. 2020 Jul 10;9:e55513.
65. Rardin MJ, et al. SIRT5 regulates the mitochondrial lysine succinylome and metabolic networks. Cell Metab. 2013;18(6):920–33.
66. Hirschey MD, et al. SIRT3 regulates mitochondrial protein acetylation and intermediary metabolism. Cold Spring Harb Symp Quant Biol. 2011;76:267–77.
67. Guo AH, et al. Sirtuin 5 levels are limiting in preserving cardiac function and suppressing fibrosis in response to pressure overload. Sci Rep. 2022;12(1):12258.
68. Koentges C, Bode C, Bugger H. SIRT3 in Cardiac Physiology and Disease. Front Cardiovasc Med. 2016;3:38.
69. Victoria Hung, et al. Proteomic mapping of cytosol-facing outer mitochondrial and ER membranes in living human cells by proximity biotinylation. eLife 6:e24463.
70. Distler AM, Kerner J, Hoppel CL. Proteomics of mitochondrial inner and outer membranes. Proteomics. 2008;8(19):4066–82.
71. MJ. P., Structure and function of ER membrane contact sites with other organelles. Nat Rev Mol Cell Biol 2016 Feb 17(2): 69–82.
72. Brown KA, et al. Nonionic, cleavable surfactant for top-down proteomics. Anal Chem. 2023;95(3):1801–4.
73. Donnelly DP, et al. Best practices and benchmarks for intact protein analysis for top-down mass spectrometry. Nat Methods. 2019;16(7):587–94.
74. Shen X, et al. Capillary zone electrophoresis-mass spectrometry for top-down proteomics. TRAC Trends Anal Chem. 2019;120:115644.
75. McCool EN, et al. Deep Top-Down Proteomics using Capillary Zone Electrophoresis-Tandem Mass Spectrometry: identification of 5700 Proteoforms from the Escherichia coli Proteome. Anal Chem. 2018;90(9):5529–33.
76. Kaulich PT, et al. Improved identification of Proteoforms in Top-Down Proteomics using FAIMS with Internal CV Stepping. Anal Chem. 2022;94(8):3600–7.
77. Gerbasi VR, et al. Deeper protein identification using Field Asymmetric Ion mobility spectrometry in top-down proteomics. Anal Chem. 2021;93(16):6323–8.
78. Guo Y, et al. Multidimensional separations in top–down proteomics. Anal Sci Adv. 2023;4(5–6):181–203.
79. Yu D, et al. Deep Intact Proteoform characterization in human cell lysate using High-pH and Low-pH reversed-phase liquid chromatography. J Am Soc Mass Spectrom. 2019;30(12):2502–13.
80. Tucholski T, et al. A top-down proteomics platform coupling serial size Exclusion Chromatography and Fourier Transform Ion Cyclotron Resonance Mass Spectrometry. Anal Chem. 2019;91(6):3835–44.
81. Tian Z, et al. Enhanced top-down characterization of histone post-translational modifications. Genome Biol. 2012;13(10):R86.
82. Simpson DC, et al. Using size exclusion chromatography-RPLC and RPLC-CIEF as two-dimensional separation strategies for protein profiling. Electrophoresis. 2006;27(13):2722–33.
83. Kaulich PT, Cassidy L, Tholey A. *Identification of proteoforms by top-down proteomics using two-dimensional low/low pH reversed-phase liquid chromatography-mass spectrometry.* PROTEOMICS, 2023. n/a(n/a): p. 2200542.
84. Xiu L, et al. Effective protein separation by Coupling Hydrophobic Interaction and Reverse Phase Chromatography for top-down proteomics. Anal Chem. 2014;86(15):7899–906.
85. Guo Y, et al. Optimization of protein-level tandem mass tag (TMT) labeling conditions in complex samples with top-down proteomics. Anal Chim Acta. 2022;1221:340037.
86. Guo Y, et al. Optimization of Higher-Energy Collisional Dissociation Fragmentation Energy for Intact protein-level Tandem Mass Tag labeling. J Proteome Res. 2023;22(5):1406–18.
87. Guo Y, et al. A benchmarking protocol for intact protein-level Tandem Mass Tag (TMT) labeling for quantitative top-down proteomics. MethodsX. 2022;9:101873.
88. Winkels K, Koudelka T, Tholey A. Quantitative top-down proteomics by Isobaric labeling with Thiol-Directed Tandem Mass tags. J Proteome Res. 2021;20(9):4495–506.
89. Chen X, et al. Quantitative proteomics using isobaric labeling: a practical guide. Genom Proteom Bioinform. 2021;19(5):689–706.
90. Sivanich MK, et al. Recent advances in isobaric labeling and applications in quantitative proteomics. Proteomics. 2022;22(19–20):2100256.

Publisher's note